
Tunable Light-guide Image Processing Snapshot Spectrometer (TuLIPSS) for Earth Observation

T.S.Tkaczyk¹, D.Alexander², J.C.Luvall³, Ye Wang¹, J. G.Dwight¹, M.E.Pawlowski¹,
R.I.Stoian¹, Shuna Cheng¹, Antoun Daou², P.Tatum³

¹ Department of Bioengineering, Rice University, Houston, Texas 77005

² Department of Physics and Astronomy, Rice University, Houston, Texas 77005,

³ NSSTC, NASA Marshall Space Flight Center, Huntsville, AL 35805.

Supported by NASA ESTO Instrument Incubator Program
NNH16ZDA001N-IIP

TuLIPSS Team

Principal Investigator: Dr. Tomasz Tkaczyk, Rice University

Co-Investigators:

Dr. David Alexander (Science-PI), Rice University

Dr. Jeffrey C. Luvall, Marshall Space Flight Center

NASA Reference Project Support

MS. Eng. Paul F. Tatum, Marshall Space Flight Center

Dr. Andrew Molthan, Marshall Space Flight Center

Dr. Walter Petersen, Marshall Space Flight Center

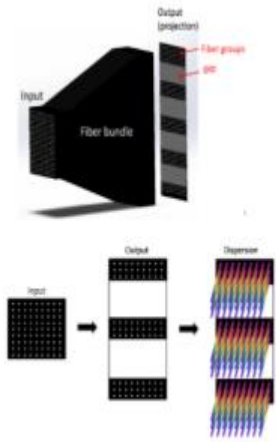
Collaborators :

Dr. Scott McIntosh, Director, High Altitude Observatory, NCAR

Dr. Thomas L Sever, Dept. of Atmospheric Sciences, Univ. of Alabama Huntsville

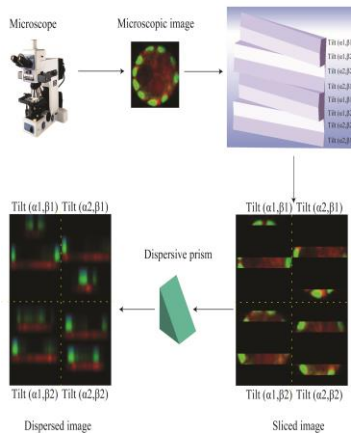
Dr. Dale A Quattrochi, Earth Science Office, NASA MSFC

Snapshot Multi / Hyperspectral Systems based on Image Re-organization

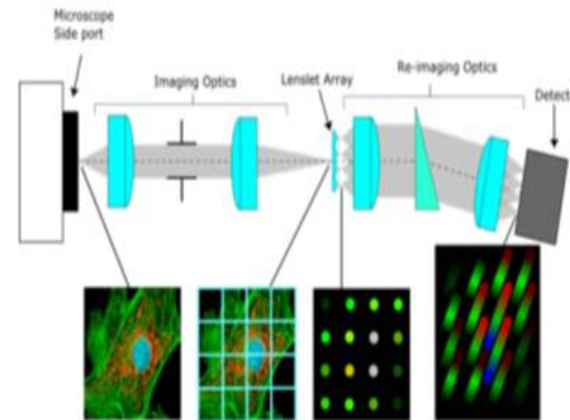


Ye Wang et al, OPTICAL ENGINEERING, Volume: 56 Issue: 8. AUG 2017

- Ye Wang et al, OPTICAL ENGINEERING, Volume: 56 Issue: 8. AUG 2017
- Biomed. Opt. Express 8, 1950-1964 (2017)
- Opt. Express 21, 13758-13772 (2013)
- Biomed. Opt. Express 4, 938-949 (2013)
- Journal of Cell Science, JOCES/2012/108258
- Journal of Biomedical Optics Letters, August 2012 • Vol. 17(8), p.080508-1
- Optical Engineering 51(11), (November 2012)
- Optical Engineering 51(4), 043203 (April 2012)
- JOURNAL OF MICROSCOPY Volume: 246 Issue: 2 Pages: 113-123, MAY 2012
- Biomed. Opt. Express 3, 48-54 (2012)
- Opt. Express 19, 17439-17452 (2011)
- Journal of Biomedical Optics, 16(05), 056005, May 2011
- Opt. Express 18, 14330-14344 (2010)
- Appl. Opt. 49, 1886-1899 (2010)
- Opt. Express 17, 12293-12308 (2009)



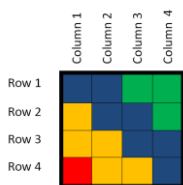
Liang Gao et al 20 July 2009 / Vol. 17, No. 15 / OPTICS EXPRESS



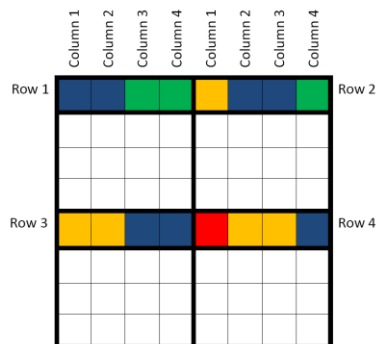
Dwight et al Biomed. Opt. Express 8, 1950-1964 (2017)

- Multi – Dimensional
 - 3D+
- Field distribution
 - Reorganizing the field of view to separate image segments
- Snapshot
 - Instantaneous acquisition
- Simple Reconstruction
 - Calibration + Image Reorganizing

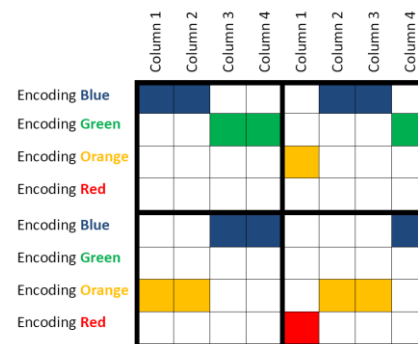
Breaking Down the Image



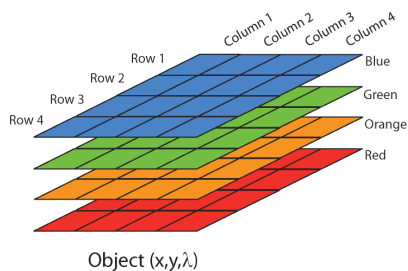
A



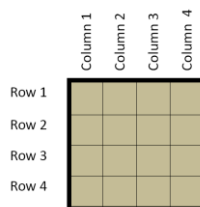
B



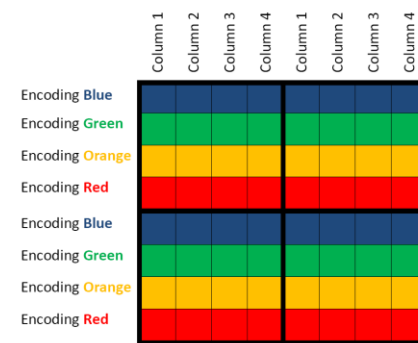
C



D



E



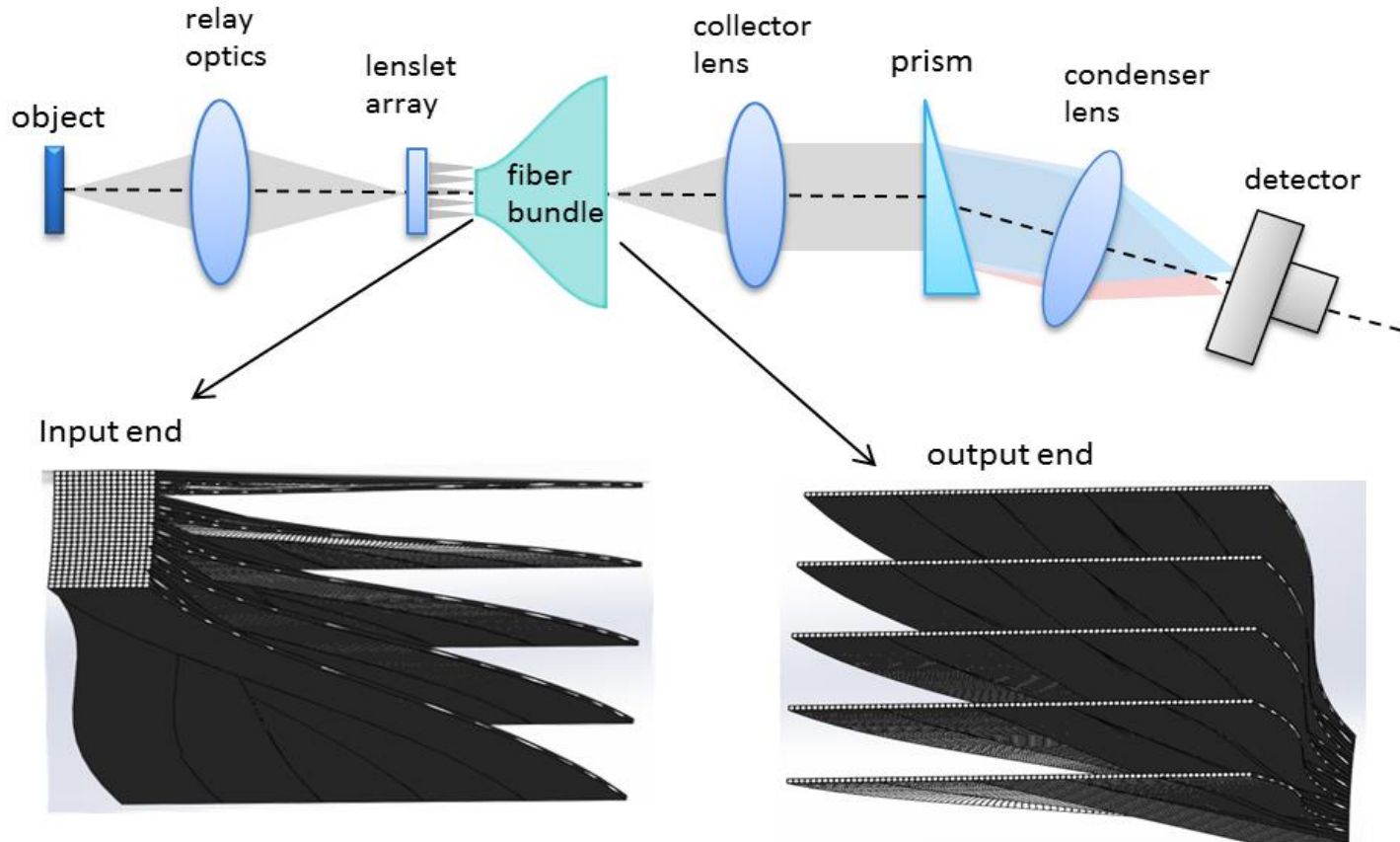
F

System Design

General Design

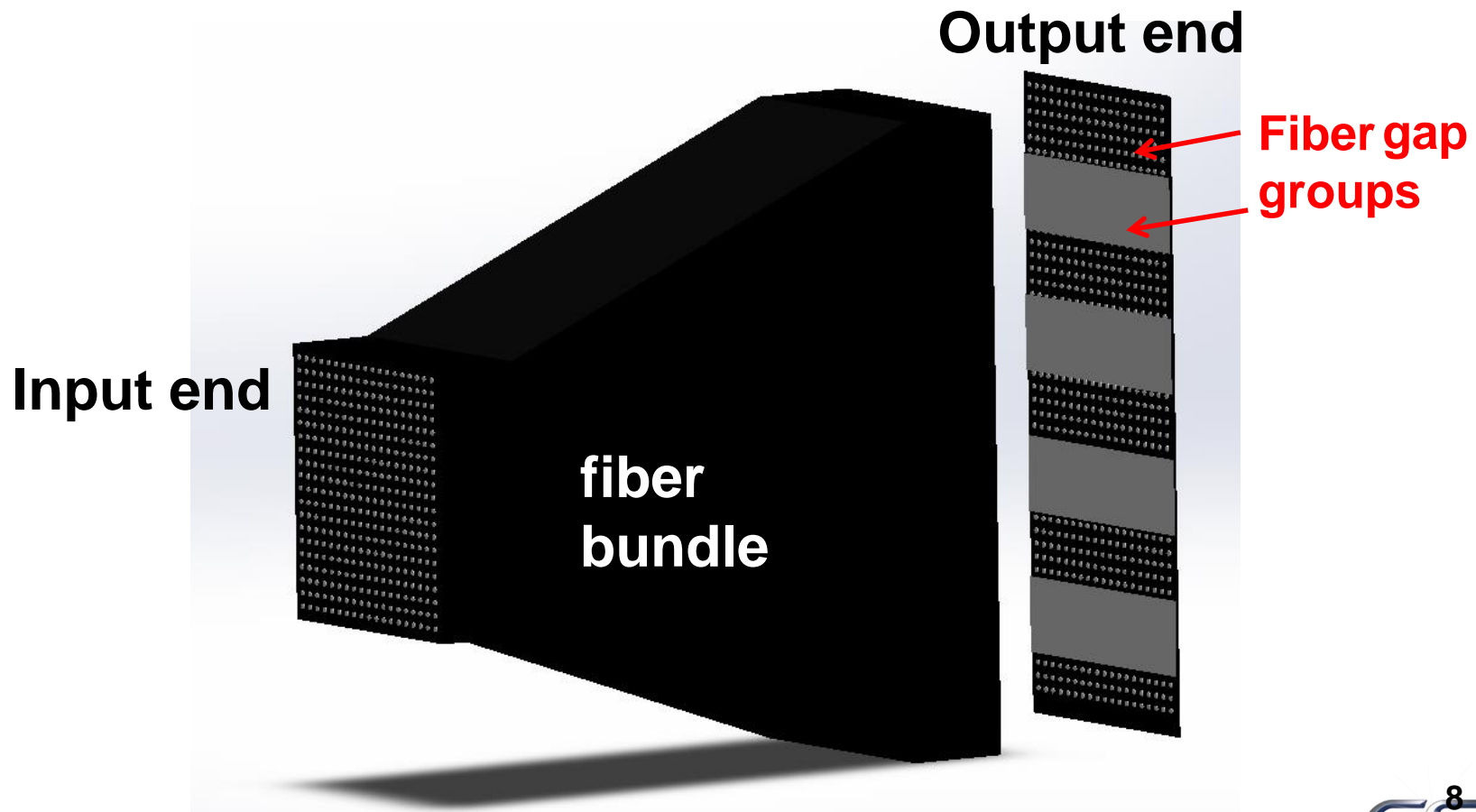
Fiber Parameters vs. System Design

General System Layout

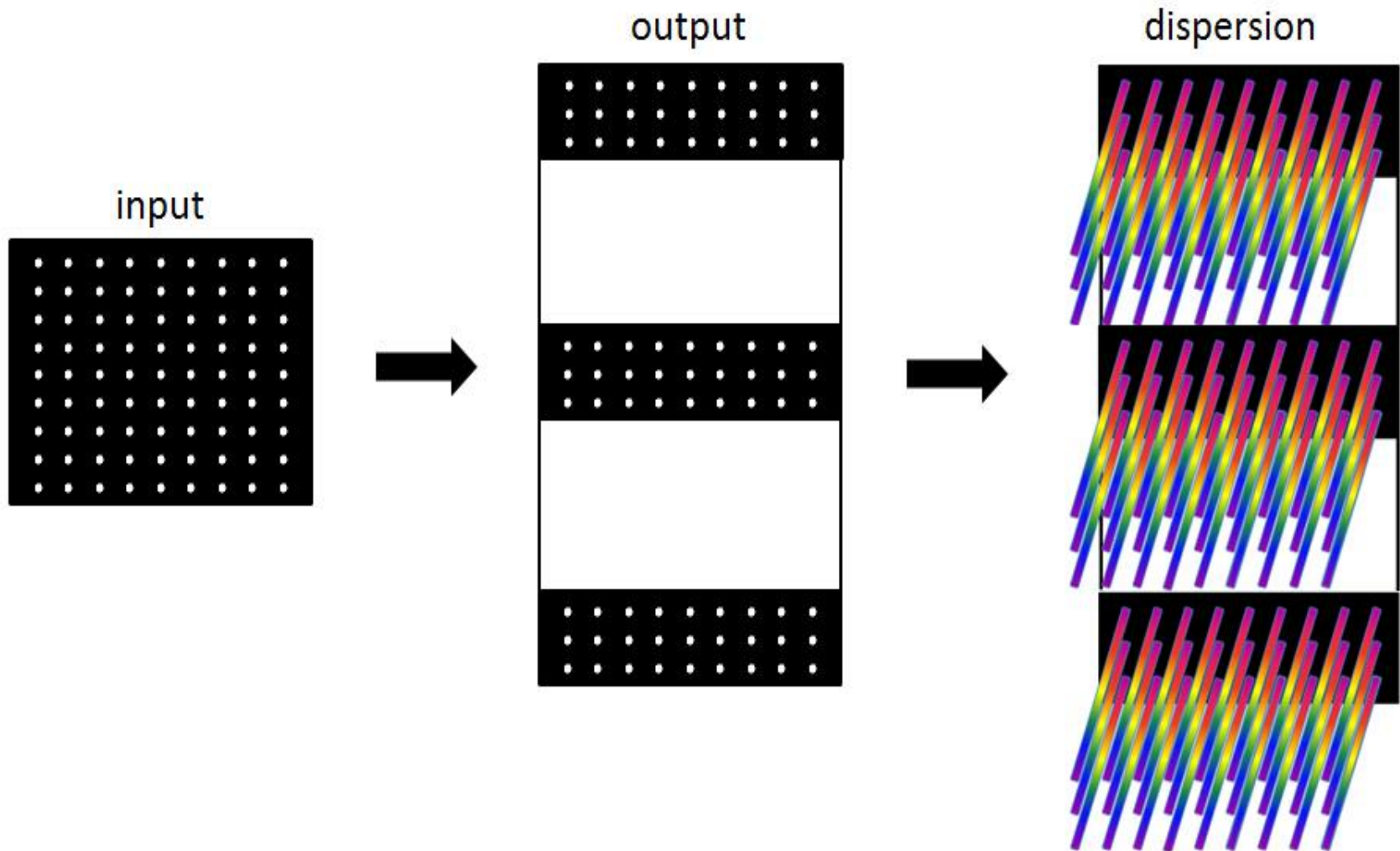


Custom Fiber Bundle System

- Prototype of a fiber-based snapshot spectrometer



General principle



Snapshot advantages

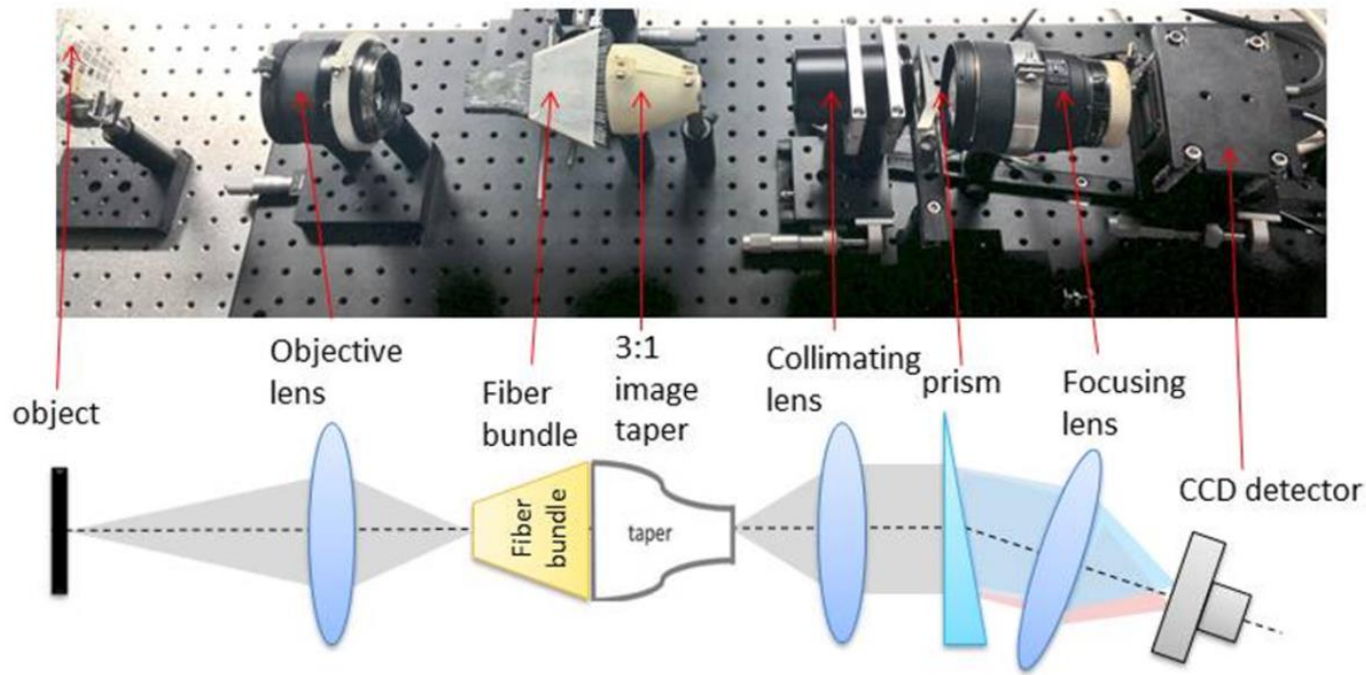
- Monitoring of fast processes
 - Range: FPA speed to end-user-specified timeframes
- Less susceptible to vibrations/movements
- 3D capability for snapshots taken at different inclinations/zenith
 - Tomography, topography
- Improvement of signal quality
 - Via scene overlap (UAV/satellite speed-dependent)
- Glint compensation
 - Via tilting capability
- Orbital scanning for imaging scenes adjacent to “along-track” direction
- Reverse gimbaling for prolonged exposure/integration time/number of images to improve signal quality and resolution for area of interest
- Gimbal scanning for extending resolution imaging/super sampling
- Predicting scene change for setting tuning parameters e.g. land to water
- Lightning detection

Tunability advantages

- Optimization of spectral resolution within a given spectral range to ascertain greater spectral detail of spectral lines
 - Change spectral range
 - Multiple high spectral resolution subsets of range
 - Different datasets for same target for analysis
 - Change spectral sampling within subset
 - Compensate for signal conditions – improvement of dynamic range
 - Change spatial sampling (trade-off)
- Increased signal collection for reduced spatial sampling in low irradiance conditions
- Filter image conjugates of scenes with both dim and bright objects via ND filters and DMDs (Digital Mirror Device)
- Target of opportunity adaptability
 - Quick adjustment for fast fly-bys
- Optimization of DATA transfer – only critical data can be collected

Major Focus of Year 1

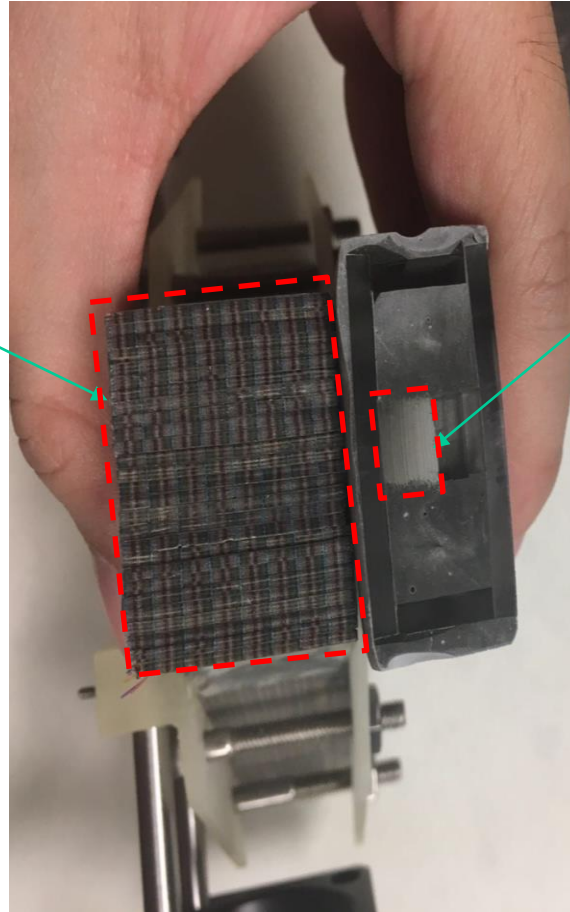
- Decrease fiber module dimensions to allow compact tunable spectrometer. The fiber module parameters drive system's design.



Proposal Prototype

Light guide Fiber bundle: input area

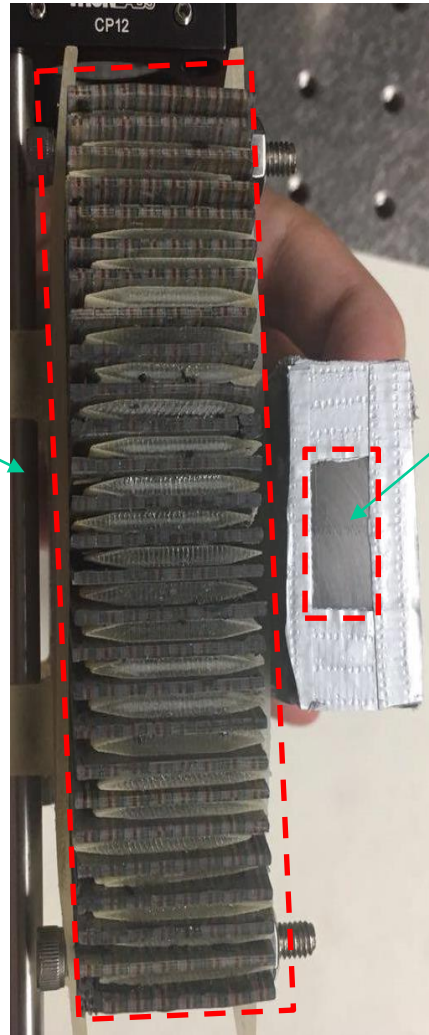
Proposal
Prototype



New
TuLIPSS

Light guide Fiber bundle: output area

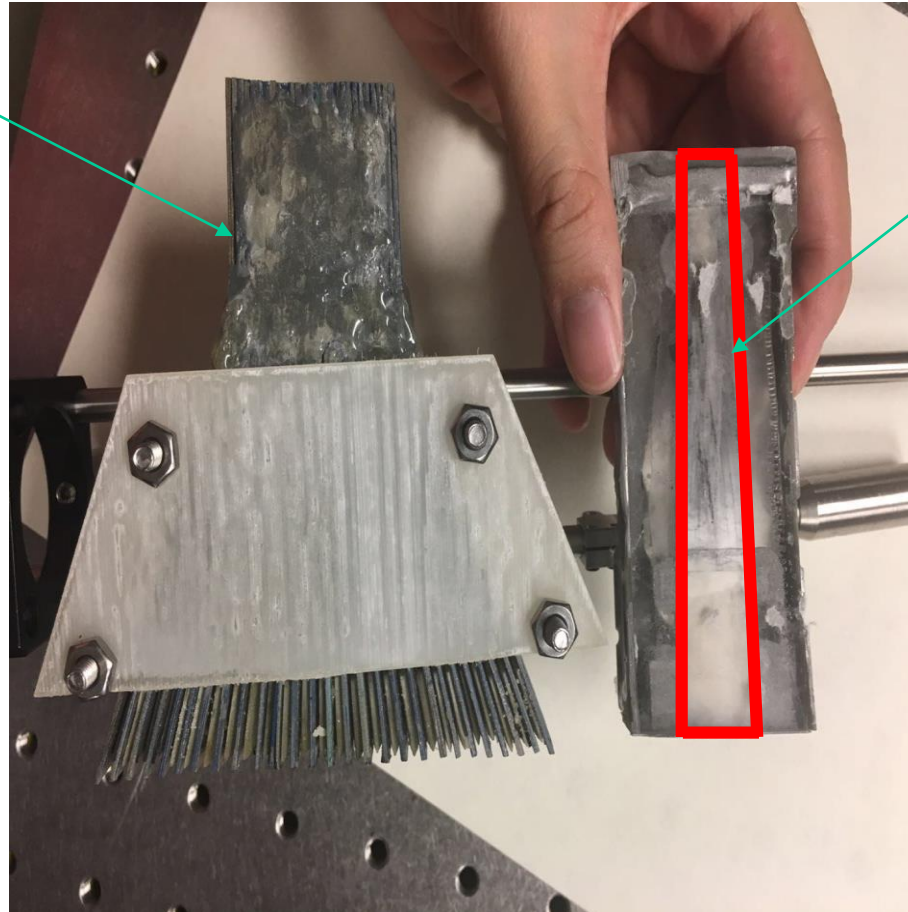
Proposal
Prototype



New
TuLIPSS

Light guide Fiber bundle

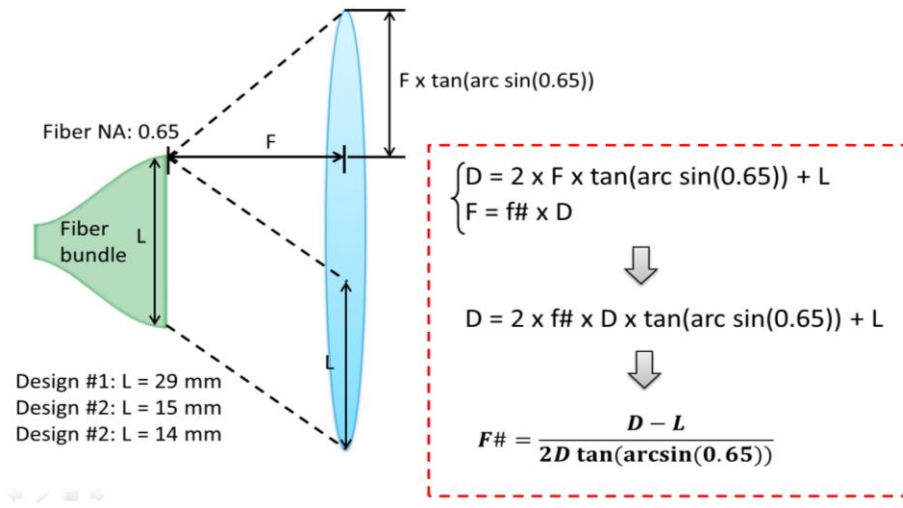
Proposal
Prototype



New
TuLIPSS

Fiber NA vs. System Design

Calculations Performed for 200x200x30 configuration



design #1
 $L = 29$ mm

D	F#
50 mm	0.25
80 mm	0.37
100 mm	0.42
150 mm	0.47

design #2
 $L = 15$ mm

D	F#
50 mm	0.41
80 mm	0.48
100 mm	0.50
150 mm	0.53

design #3
 $L = 14$ mm

D	F#
50 mm	0.42
80 mm	0.48
100 mm	0.50
150 mm	0.53

Light Loss for NA=0.64

Loss = 25%

D	F#
50 mm	0.50
80 mm	0.57
100 mm	0.59
150 mm	0.62

Loss = 50%

D	F#
50 mm	0.65
80 mm	0.72
100 mm	0.74
150 mm	0.77

Loss = 75%

D	F#
50 mm	0.99
80 mm	1.06
100 mm	1.08
150 mm	1.11

Loss = 80%

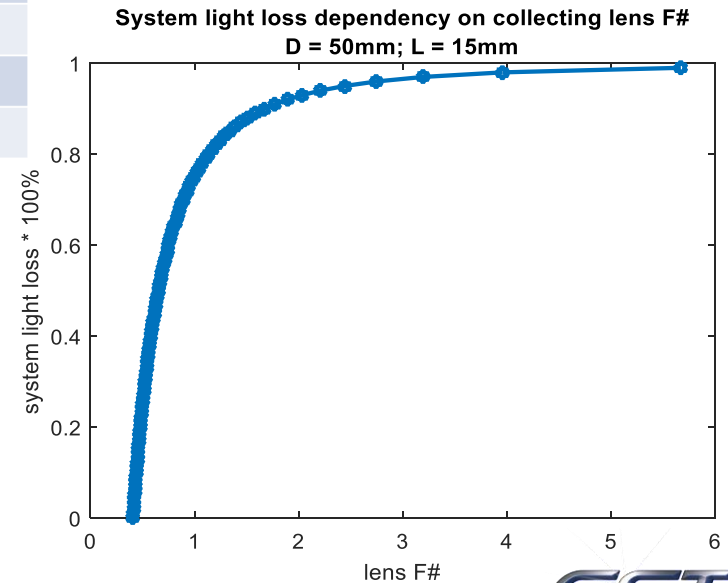
D	F#
50 mm	1.13
80 mm	1.20
100 mm	1.22
150 mm	1.25

Loss = 85%

D	F#
50 mm	1.33
80 mm	1.40
100 mm	1.42
150 mm	1.45

Loss = 90%

D	F#
50 mm	1.67
80 mm	1.74
100 mm	1.76
150 mm	1.79



Light Loss vs. Fiber NA and F#

NA = 0.65

D	F#
50 mm	0.41
80 mm	0.47
100 mm	0.50
150 mm	0.52

NA = 0.55

D	F#
50 mm	0.53
80 mm	0.62
100 mm	0.65
150 mm	0.68

NA = 0.45

D	F#
50 mm	0.69
80 mm	0.81
100 mm	0.84
150 mm	0.89

NA = 0.35

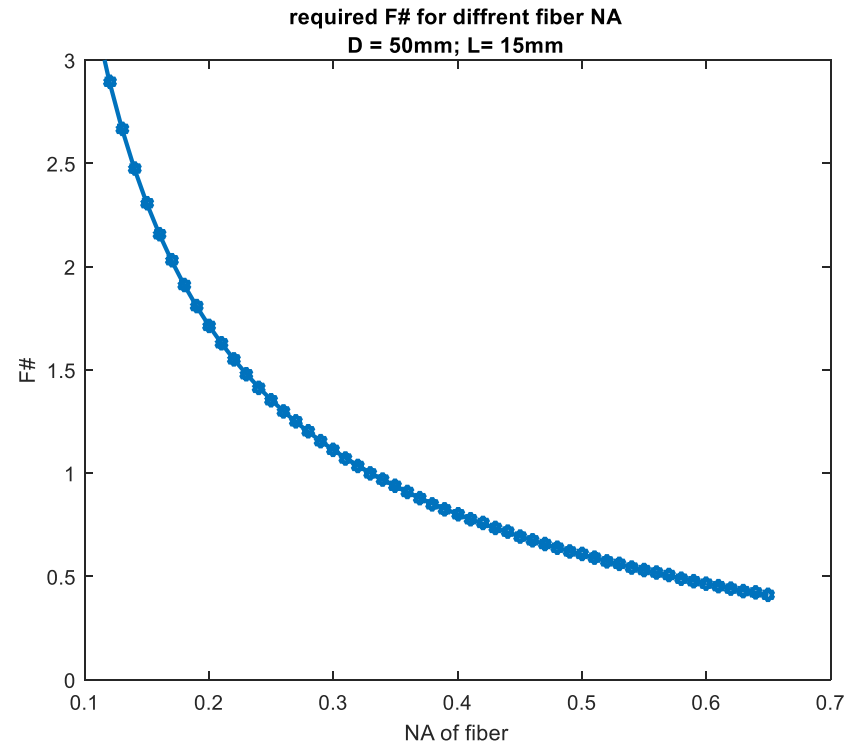
D	F#
50 mm	0.94
80 mm	1.09
100 mm	1.14
150 mm	1.20

NA = 0.25

D	F#
50 mm	1.36
80 mm	1.57
100 mm	1.65
150 mm	1.74

NA = 0.15

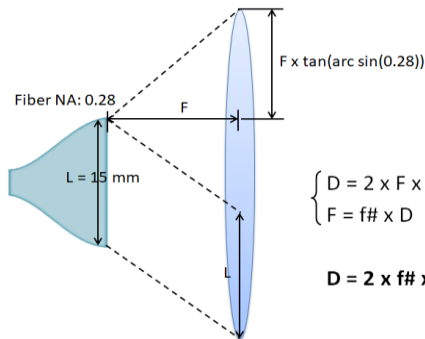
D	F#
50 mm	1.36
80 mm	1.57
100 mm	1.65
150 mm	1.74



Solutions to maximize light collection

- Lower NA of the fiber
- Lenslets at fiber tips
- Custom Optimized Fresnel Lens

TuLIPSS system lens requirements for
0.28 NA



$$\begin{cases} D = 2 \times F \times \tan(\arcsin(0.28)) + L \\ F = f\# \times D \end{cases}$$

$$D = 2 \times f\# \times D \times \tan(\arcsin(0.28)) + L$$

- 0% loss:

D	F
30 mm	26mm
50 mm	60mm
80 mm	112mm
100 mm	145mm

200 x 200 x 30
L = 15 mm

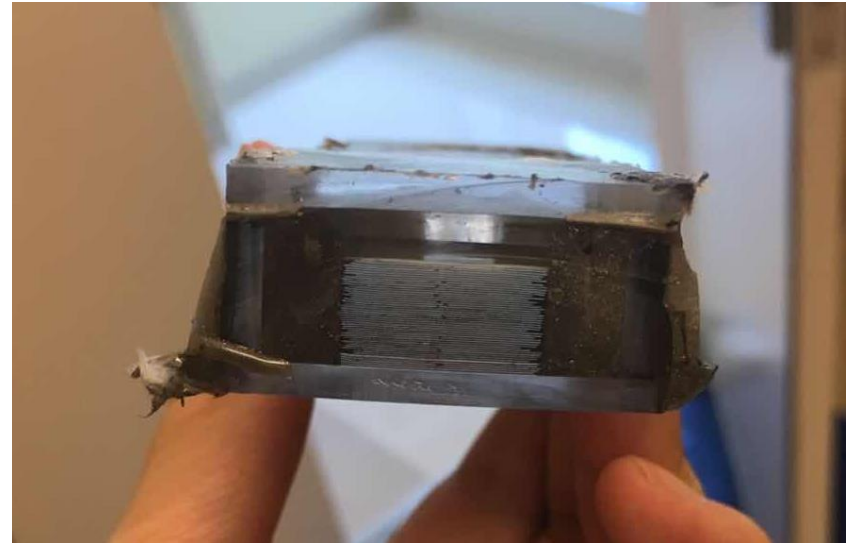


Fresnel Lens

Assembly and Polishing

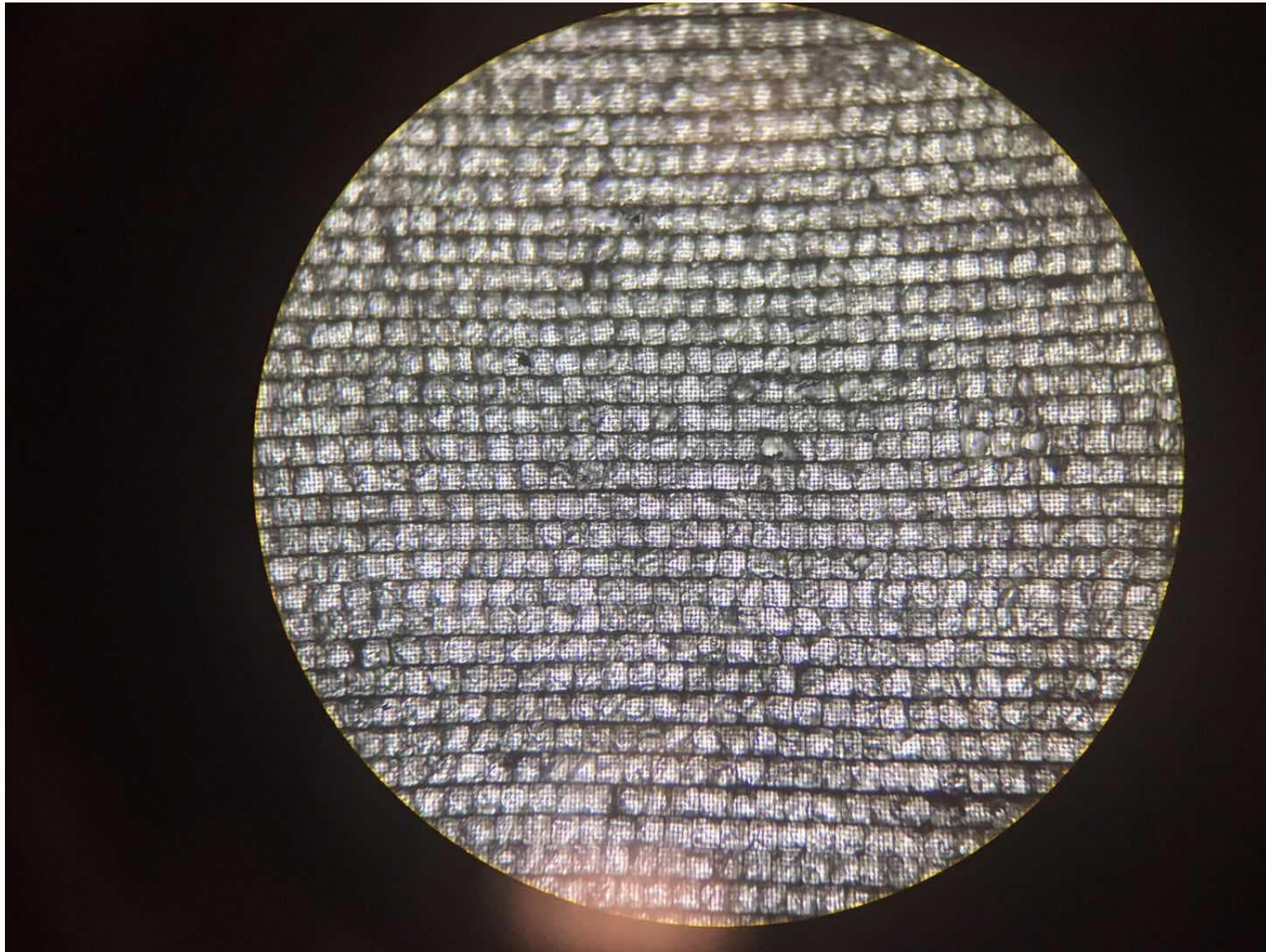


Input

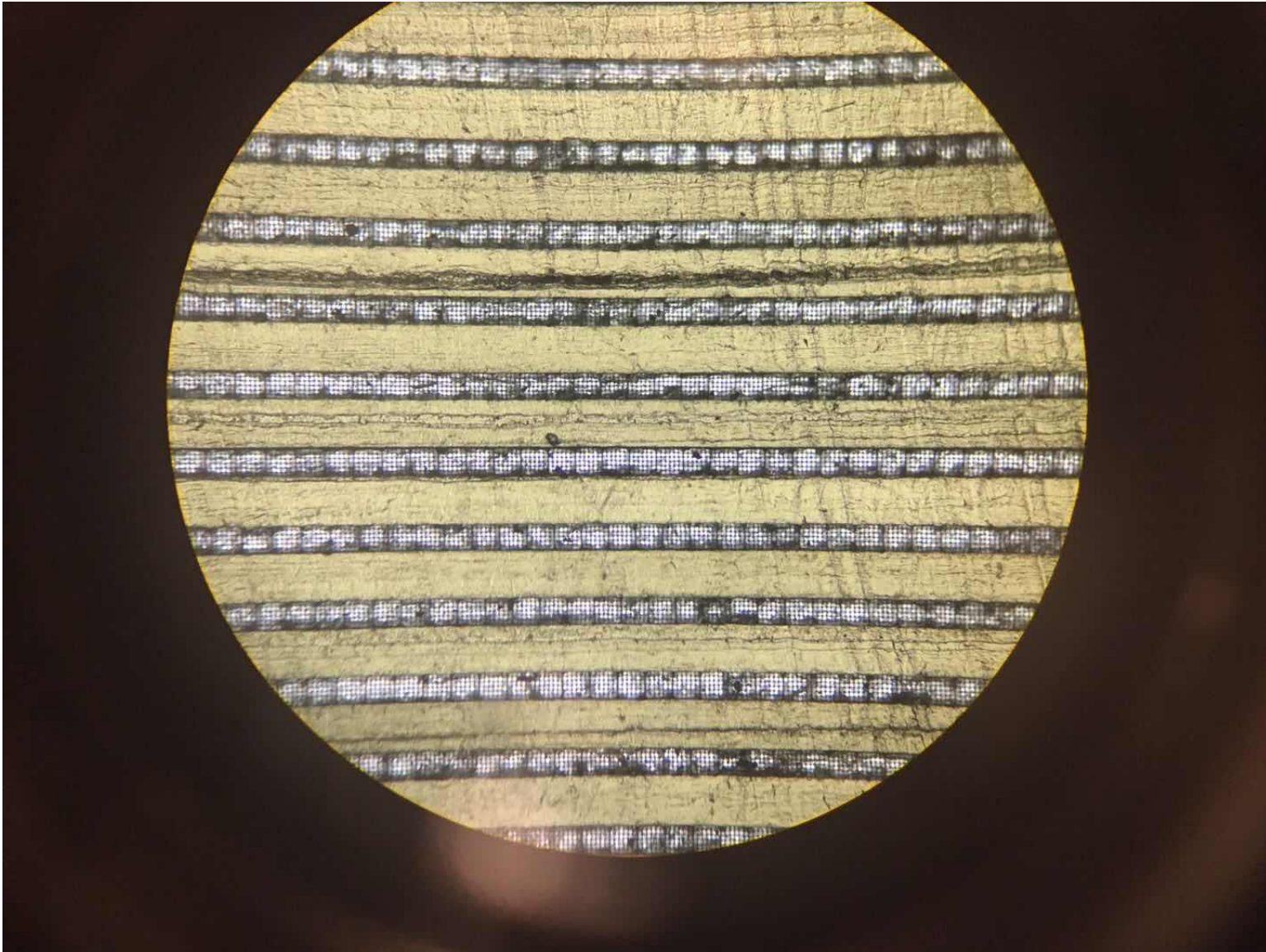


Output

LIP Input – Before Polishing

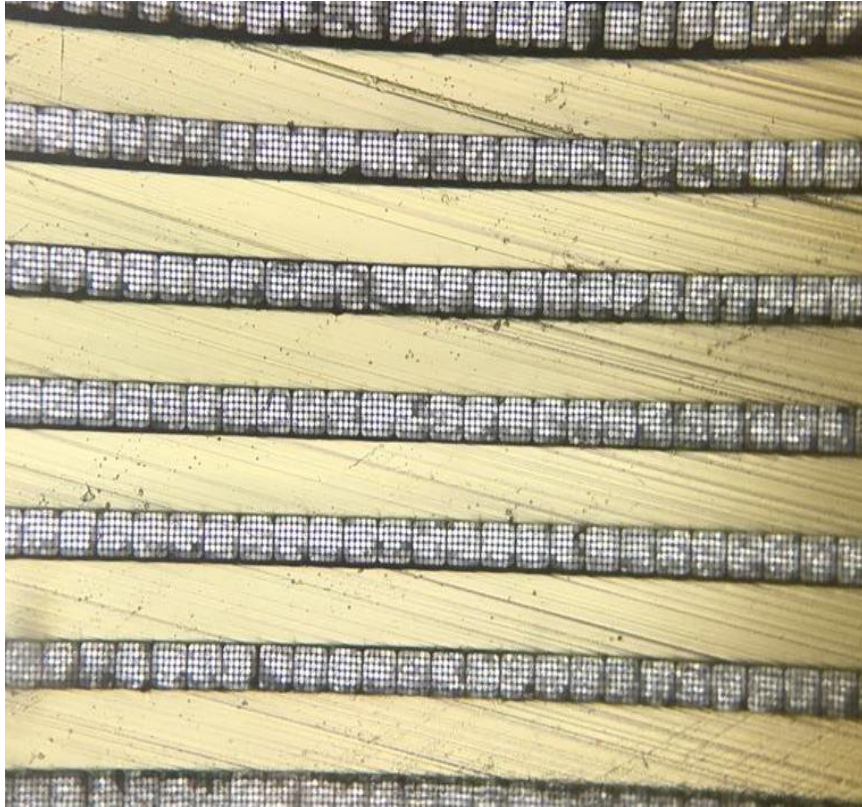


LIP Output – Before Polishing



Water polish

before

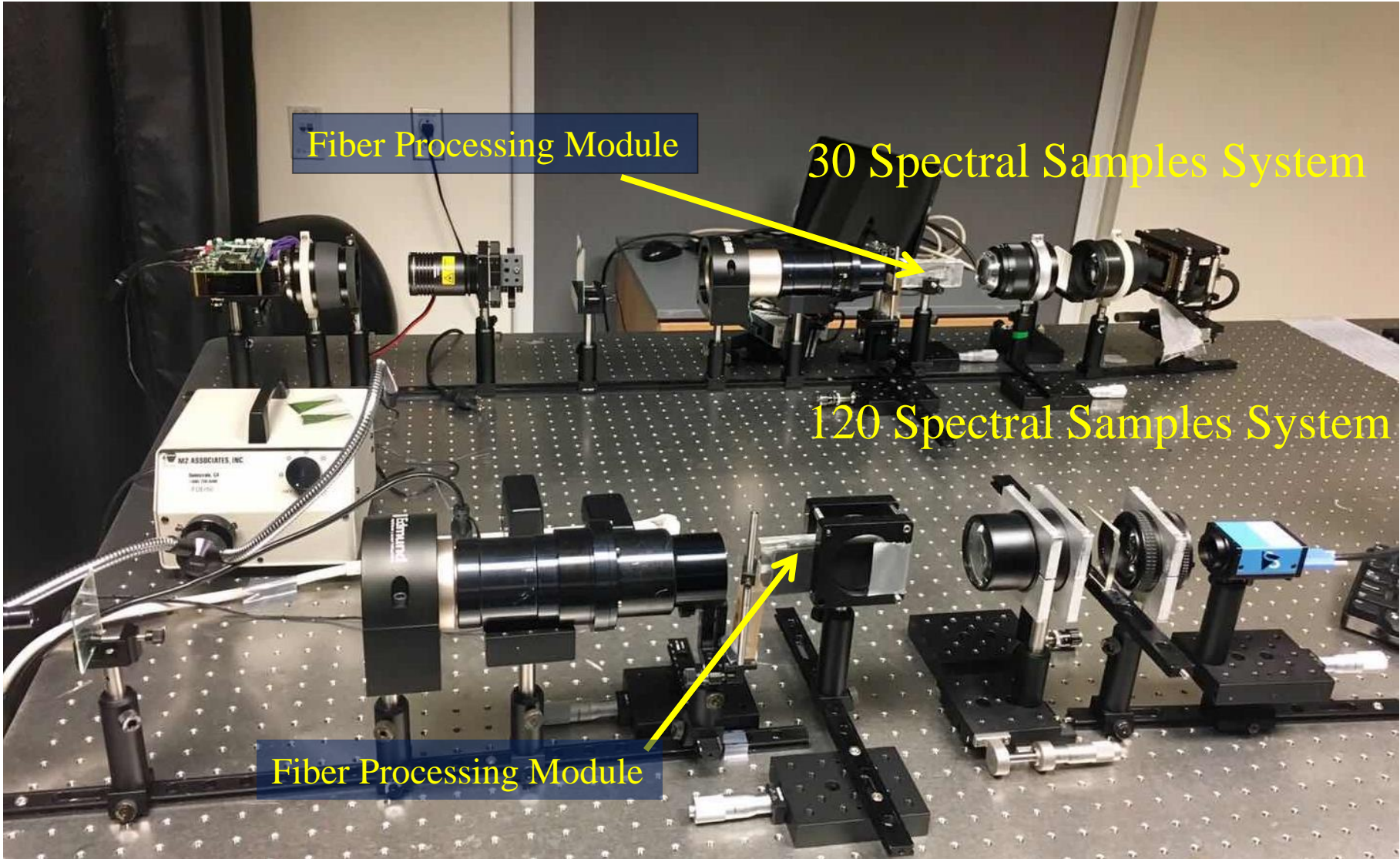


after



Polishing process significantly improves fiber face quality
Longer polishing time and change of polishing material allows
achieving necessary <10 nm roughness

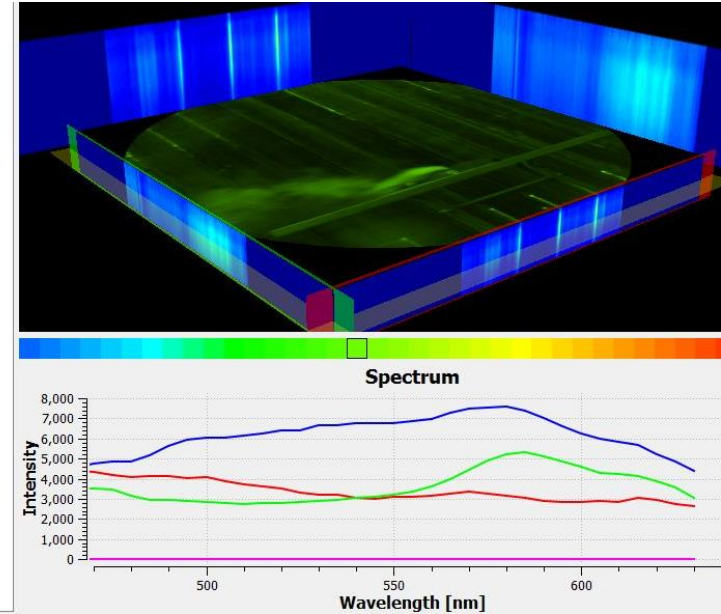
Benchtop Prototypes



System Level results

SNAP-IMS Reference Results

Gas Detection



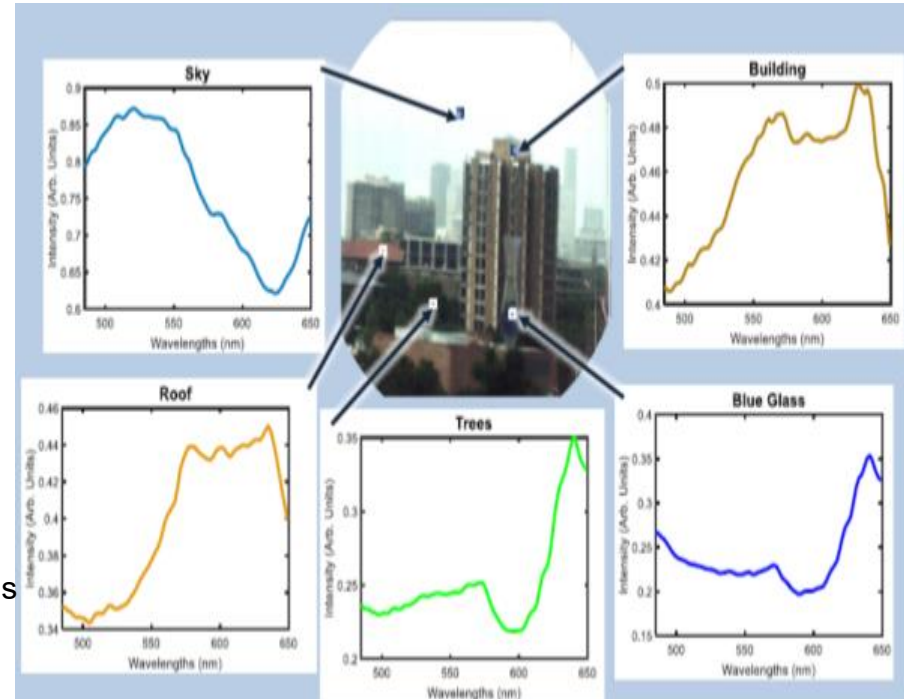
RT.Kester, N.Bedard, TS. Tkaczyk, Image mapping spectrometry – a novel hyperspectral platform for rapid snapshot imaging, Proc. of SPIE Vol. 8048, April 2011

Mirror Based – compact image slicing/mapping system – cont.



J.Dwight et. al, poster presentation at Hypsiri Workshop, Caltech, October 2017

- A cost effective platform for environmental sensing applications that include monitoring water quality, land use, air pollution, vegetation and agriculture.
- Small size, power, and weight of payloads allows for a wider range of applications, incorporation of additional instrumentation or the augmentation of flight parameters such as altitude, distance and duration.
- System demonstrates high light-throughput.
- Hyperspectral datacubes can be acquired at 1/500 sec to 1/100 sec, eliminating motion artifacts
- Applications include monitoring plant pigmentation, vegetation state, leak detection at petrochemical plants, and urban sustainability, lightning etc.



J.Dwight et. al, poster presentation at Hypsiri Workshop, Caltech, October 2017

Supported by NASA Cooperative Agreement Notice (CAN) No. NNM16567212C for Dual-Use Technology Development at MSFC

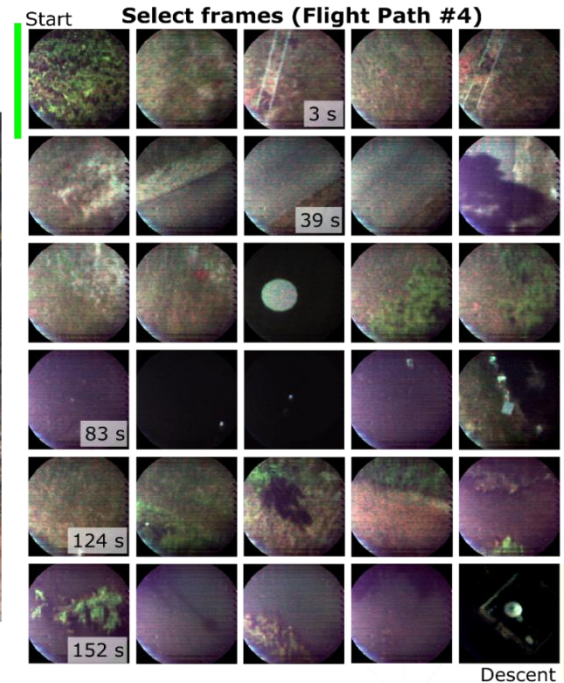
Mirror Based – compact image slicing/mapping system – cont.



Proc. SPIE, April 2018, Orlando, FL
 Defense and Commercial Sensing 2018

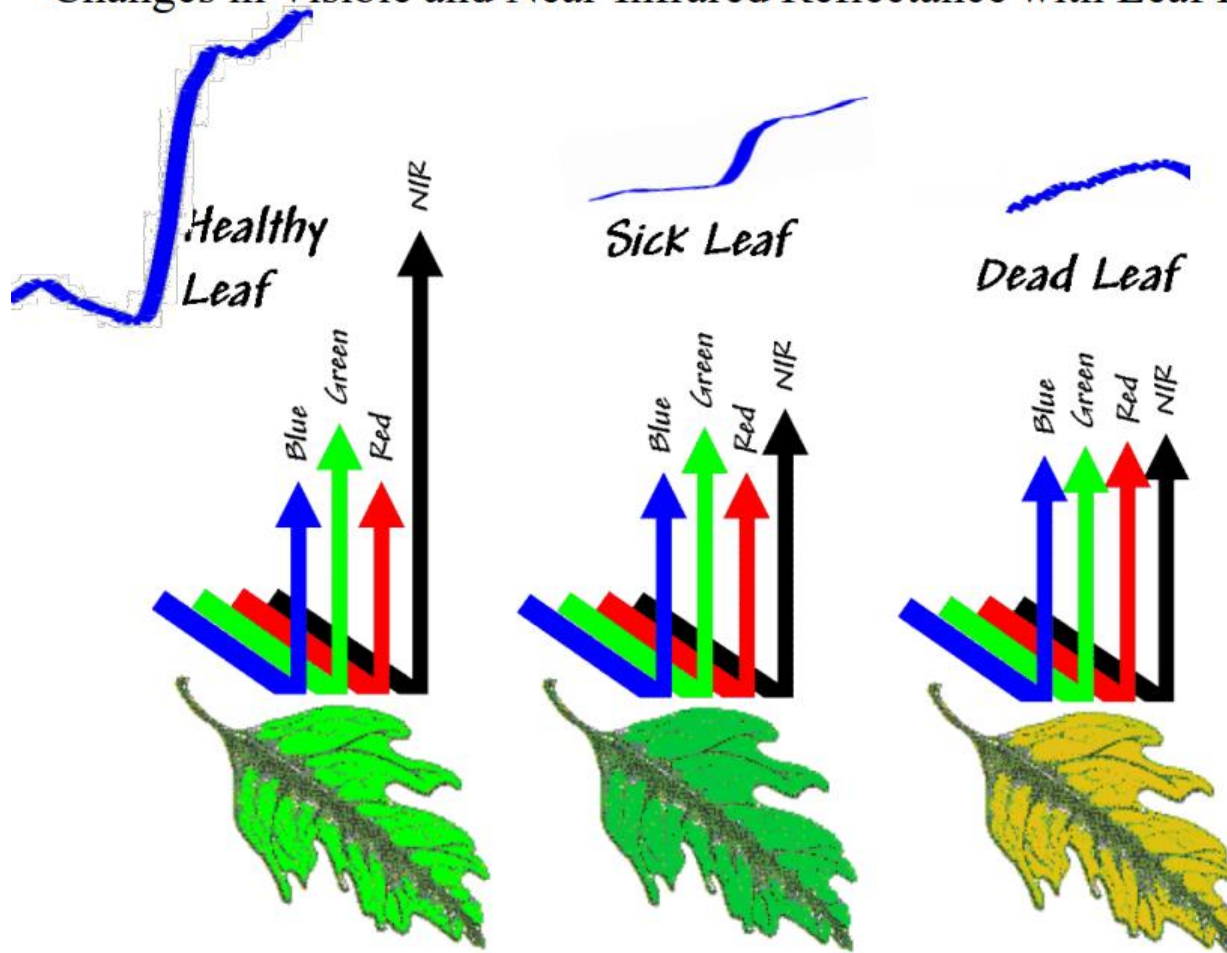
Photos taken of the flight. Shown is the SNAP-IMS with its UAV mounting bracket (left), the SNAP-IMS/UAV integration (center), and the drone midflight with the SNAP-IMS (right).

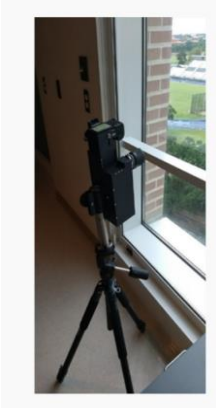
Flight Path #4



The flight path of #4 with select frames and their corresponding times

Changes in Visible and Near-Infrared Reflectance with Leaf Health





Canopy							
Specific observational targets	Line centroid(s) [nm]	Sub-band [nm]	Spectral sampling (no of samples in sub-band)	Spatial resolution	Experiment Type	SNR	Snapshot, Tunability, and Other Features of TuLIPSS
Leaf Chlorophyll Content at the Canopy Scale (Triangular Greenness Index-TGI)	670 550 480	630-690 520-600 450-520 or Broadband 400-700	24 32 20 100	<30	Reflectance $TGI = -0.5[(670 - 480)(R_{670} - R_{550}) - (670 - 550)(R_{670} - R_{480})]$	TBD	Spectral sampling change (Tunability) or Bandwidth Change (Tunability)

Wilted plant

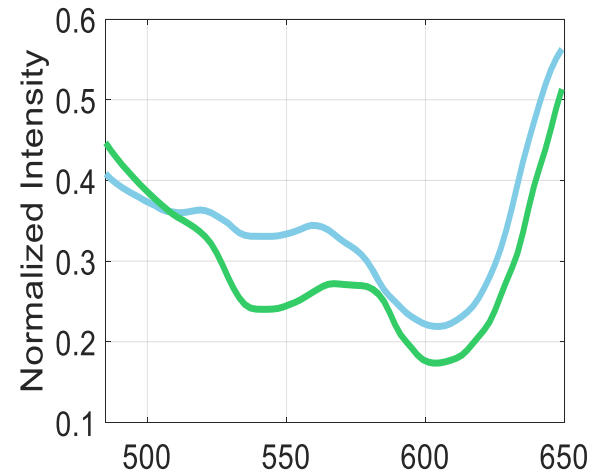


TGI value = 12.6

Watered plant



TGI value = 21.7

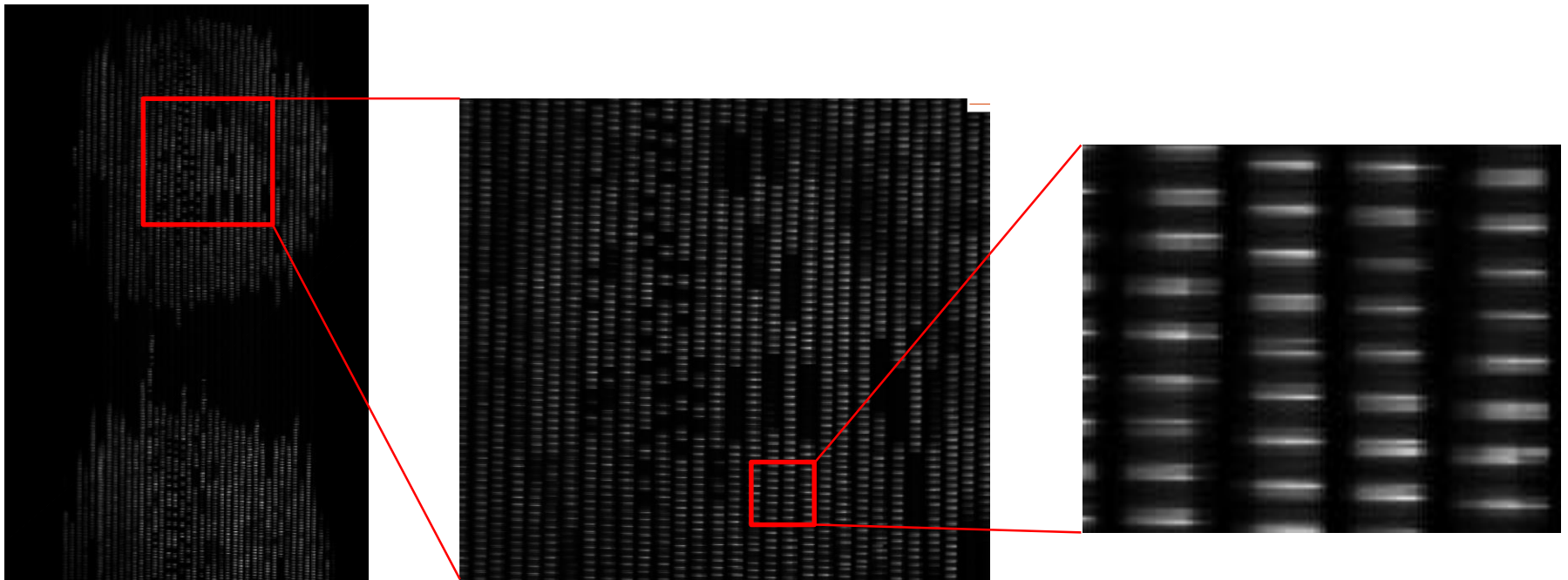


Wilted plant

Watered plant

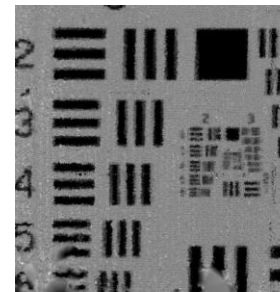
TuLIPSS Imaging

USAF 1951 Resolution Target



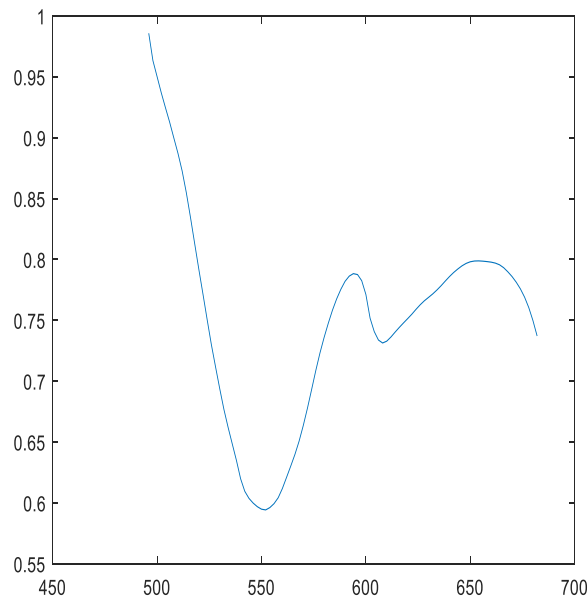
Raw Images

Reconstructed Image



TuLIPSS Imaging Results

- Leaf
 - Averaged absorbance spectrum



TuLIPSS Functionality vs Science Applications

Science Applications

Chlorophyll and Xanthophyll (carotenoids) monitoring via vegetation indexes

1. Precision Agriculture – Nitrogen and water stress detection within hours [ref. 1, 2, 3]

- **TuLIPSS advantages: Tuning via band-pass filters or spectral sampling over VIS/NIR detector spectral range**
- Centroids:
 - 539 nm (e.g. Xanthophyll fluorescence - sun flower canopy) [ref. 2]
 - 690 nm, 740 nm – Chlorophyll fluorescence [ref. 3]
- Band-pass filter bandwidth (sub-windows) ca. 100 (Xanthophyll) or 200 (Chlorophyll), spectral sampling per sub-windows: 10, 20, respectively

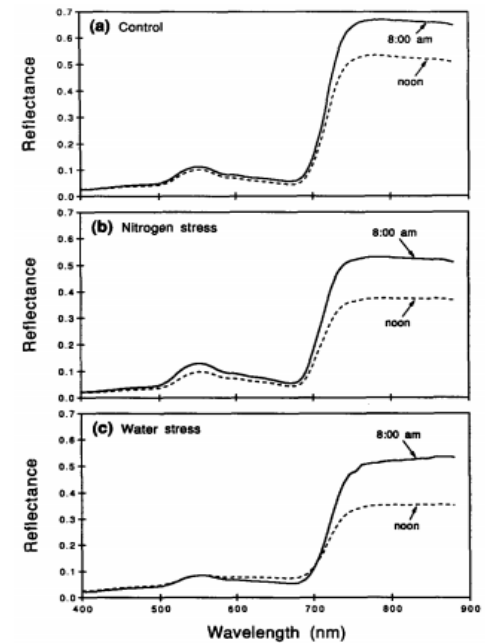
2. Precision Agriculture – Vegetation senescence

(via plant senescence reflectance index, PSRI) [ref. 4]

- **TuLIPSS advantages: Tuning via or spectral sampling over VIS/NIR detector spectral range**
- Centroids:
 - 678, 500, 750 nm
- Sampling across 400 – 750 nm: 250 samples (effective spectral resolution 1.4 nm)

3. Photochemical reflectance, normalized difference vegetation and other indexes for forest canopies [ref. 5]

- **TuLIPSS advantages: Tilting capability (snapshot) and tuning via spectral sampling across VIS/NIR**
- **Other snapshot advantages**
 - Cross-track scanning for imaging scenes adjacent to “along-track” direction
 - Increasing survey area
- Centroids:
 - 440, 531, 570, 680, 694, 700, 715, 726, 734, 740, 747, 750, 760, 800 nm
- Number of samples: 250 per 400-1000 nm



Chlorophyll and Phycocyanin detection and measurement - Algal Blooms and Phycocyanin colonies

1. Algae identification and algae growth monitoring [ref. 6]

- **TuLIPSS advantage: Spectral sampling change and bandwidth change (with band-pass filter) (tunability) and tilting for sun glint correction (snapshot)**
 - **Other snapshot advantages**
 - Cross-track scanning for imaging scenes adjacent to “along-track” direction
 - Increasing survey area
 - Mitigate cloud cover issues
- centroid line: 700 nm (monitoring)
- sub-window: 650-760 nm (w/ band-pass filter)
- Number of samples in sub-window: 100 (ca. 1 nm effective spectral resolution)

2. Measurement of cyanobacterial phycocyanin concentration [ref. 7]

- **TuLIPSS advantage: Bandwidth change (tunability) and tilting for sun glint correction (snapshot)**
 - **Other snapshot advantages**
 - Cross-track scanning for imaging scenes adjacent to “along-track” direction
 - Increasing survey area
 - Mitigate cloud cover issues
- Centroids: 620, 665, and 708 nm
- Sub-windows: +/-50nm per centroid
- Number of samples in sub-windows spectra: 101 (effective resolution 1 nm)

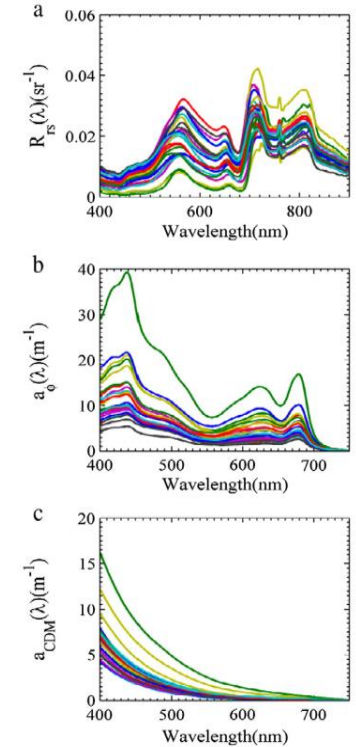
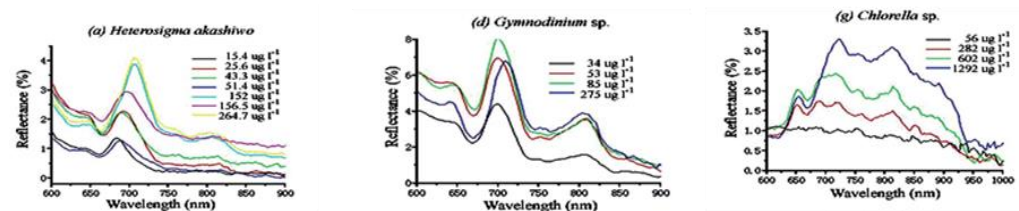


Fig. 1. (a) $R_{rs}(\lambda)$ spectra collected from aquaculture ponds in July 2010 and April 2011. (b) measured phytoplankton absorption coefficients, $a_0(\lambda)$, using filter-pad technique, and (c) measured $a_{CDM}(\lambda)$.



Total suspended solids (TSS)

1. Estimation of TSS [ref. 8]

- **TuLIPSS advantage: bandwidth selection [ref. 8] and tilting for sun glint correction (snapshot)**
- Centroids: 645 and 859 nm, sub-bands: 614 – 681 nm, 820-902 nm
- Number of samples in sub-windows: 10 (effective resolution 8 – 9 nm)

2. Study of suspended particulate matter in rivers [ref. 9]

- **TuLIPSS advantages: tilting capability for sun glint correction (snapshot)**
- Centroids: 443, 483, 561, 655, 855 nm
- Number of samples in broad band spectra: 250 (effective resolution 2.4 nm)

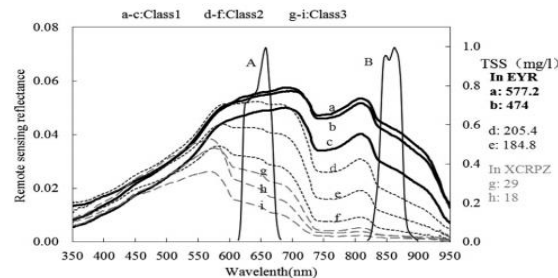


Fig. 2. The relationship between reflectance of MODIS 250-m Rrs(B1) and TSS (mg/l). The reflectance of MODIS 250-m Rrs(B1) is less than 0.025 when TSS is below ~31 mg/l (N = 26), and reflectance of MODIS 250-m Rrs(B1) is greater than 0.025 when TSS is above ~31 mg/l (N = 34).

Atmospheric gas measurement

1. NO₃ measurement [ref. 10]

- **TuLIPSS advantage: Bandwidth change – tunability around lines of interest (e.g. band-pass filters) and increased SNR (via pixel binning)**
- Centroid line: 662 nm (absorption cross-section)
- Sub-window: 640 – 680 nm
- Number of samples in sub-window: 250 (better than 0.2 nm resolution)

2. O₂ measurement [ref. 11]

- **TuLIPSS advantage: Bandwidth change – tunability around lines of interest (e.g. band-pass filters) and increased SNR (via pixel binning)**
- Centroid line: 760 nm [ref. 11]
- Sub-window: 740-780 nm
- Number of samples in sub-window: 250 (better than 0.2 nm resolution)

1. Disaster monitoring/mitigation (augmented with TIR)

- Volcanic CO₂ absorption features at 1270 nm and 1610 nm [ref. 12]
- Tuning capability:
 - centroid wavelength and bandwidth for each absorption line (band-pass filter-based tuning – coarse tuning) - +/- 75 nm
 - number of samples – (fine tuning)
 - TuLIPSS potential: 250 samples or 0.4 nm resolution (compared to 10 nm resolution in MODTRAN simulation)

2. Synoptic Measurements in Urban Landscape: Normalized Difference Built-up Index (NDBI) [ref. 13] (augmented with TIR)

- No centroids, sub-windows: NIR = 760-900 nm and SWIR = 1550-1750 nm
- $$NDBI = \frac{SWIR - NIR}{SWIR + NIR}$$

- Decreasing bundle dimensions (below 1 inch input) – smaller individual fiber diameter (10 microns and below)
- Optimizing throughput – fiber NA and coupling (lenslet array)
- Increasing spatial sampling (targeted 400x400)
- Elastic tuning (1-2 second mode switching) of fiber distance
 - Mechanical actuators
 - Magnetic
 - Pneumatic
- Dispersion and bandwidth tuning (selection of sub-bands and spectral sampling)
- ROI dynamic range tuning

– Field distribution techniques

- Can increase system throughput and enable fast imaging or better SNR
- Allow Optimizing DATA transfer
- They require limited data reconstruction
- Several hardware options are available for further developments

- [ref. 1] *Hyperspectral mapping of crop and soils for precision agriculture*, Michael, L., W., Susan, L., U., Pablo, Z.-T., Alicia, P.-O., and Vern, C., V., 2006, Proc. of SPIE, 6298, 1-15
- [ref. 2] *A narrow-waveband spectral index that tracks diurnal changes in photosynthetic efficiency*, J., A., Gamon, J., Peñuelas, and C., B., Field, 1992, Remote Sensing of Environment, 41, 35-44
- [ref. 3] *Simple reflectance indices track heat and water stress-induced changes in steady-state chlorophyll fluorescence at the canopy scale*, S., Z., Dobrowski, J., C., Pushnik, P., J., Zarco-Tejada, and S., L., Ustin, 2005, Remote Sensing of Environment, 97, 403–414
- [ref. 4] *Non-destructive optical detection of pigment changes during leaf senescence and fruit ripening*, Mark, N., M., Anatoly, A., G., Olga, B., C., and Victor, Y., R., 1999, PHYSIOLOGIA PLANTARUM, 106, 135-141
- [ref. 5] *Natural and stress-induced effects on leaf spectral reflectance in Ontario species*, Gina, H., M., Thomas, L., N., Denzil, I., Paul, H., S., Pablo, J., Z.-T., and John, R., M., 2000, Forest research report, ISSN 0381-3924
- [ref. 6] *The relationship of chlorophyll-a concentration with the reflectance peak near 700 nm in algae-dominated waters and sensitivity of fluorescence algorithms for detecting algal bloom*, Zhao, D., Z., Xing, X., G., Liu, Y., G., Yang, J., H., Wang, L., 2010, Int. J. Remote Sens., 31, 39–48
- [ref. 7] *Quantifying cyanobacterial phycocyanin concentration in turbid productive waters: A quasi-analytical approach*, Sachidananda, M., Deepak, R., M., Zhongping, L., and Craig, S., T., 2013, Remote Sensing of Environment, 133, 141–151
- [ref. 8] *Estimating wide range Total Suspended Solids concentrations from MODIS 250-m imageries: An improved method*, Shuisen, C., Liusheng, H., Xiuzhi, C., Dan, L., Lin, S., and Yong, L., 2015, ISPRS Journal of Photogrammetry and Remote Sensing, 99, 58-69
- [ref. 9] *Using Landsat 8 data to estimate suspended particulate matter in the Yellow River estuary*, Zhongfeng, Q., Cong, X., William, P., Deyong, S., Shengqiang, W., Hui, S., Dezhou, Y., and Yijun, H., 2016, Journal of Geophysical Research, 122, 276-290
- [ref. 10] *Determination of Inlet Transmission and Conversion Efficiencies for in Situ Measurements of the Nocturnal Nitrogen Oxides, NO₃, N₂O₅ and NO₂, via Pulsed Cavity Ring-Down Spectroscopy*, Hendrik, F., William, P., D., Steven, J., C., and Steven S., B., 2008, Anal. Chem., 80, 6010-6017
- [ref. 11] *Experimental Line Parameters of the Oxygen A Band at 760 nm*, L., R., Brown and C., Plymate, 2000, Journal of Molecular Spectroscopy, 199, 166-179
- [ref. 12] https://hyspiri.jpl.nasa.gov/downloads/2013_Symposium/day2_am/hyspiri_symposium_2013_buongiorno.pdf
- [ref. 13] *Remote Sensing of the Environment: An earth resource perspective*, Jensen, J., R., 2000, p.417